Properties of a tunnel point contact between aluminum and the superconducting amorphous alloy $NiZr_2$

V. F. Gantmakher, A. A. Golubov, and M. V. Osherov

Institute of Solid State Physics, USSR Academy of Sciences
(Submitted 21 April 1989)
Zh. Eksp. Teor. Fiz. **96**, 1435–1443 (October 1989)

The I-V characteristics of a tunnel point contact between aluminum and an amorphous ribbon resembling $NiZr_2$ in composition differ qualitatively from those of ordinary tunnel junctions between a superconductor and a normal metal. It is demonstrated that the observed curve shapes cannot be explained by accounting solely for one-particle tunneling in conditions of the proximity effect. This is followed by a qualitative discussion of a model in which the current rise at the potential eV equal to the gap width $\Delta(T)$ is generated by two-particle electron tunneling through the intermediate state which is manifested as a Cooper pair on the Fermi-level in the thin superconducting layer produced in the aluminum by the proximity effect. The current flowing through the contact will cause a breakdown of superconductivity in the vicinity of the contact at voltages exceeding the gap width. Smallness of the junction plays a decisive role both in inducing superconductivity for $eV < \Delta$ and in its breakdown for $eV > \Delta$.

1. INTRODUCTION

The classical I–V characteristic of a tunnel junction between a superconductor and a normal metal (an *S–I–N*-characteristic; see, for example, Ref. 1) is not always observed. For example quasiparticle tunneling from the normal metal accompanied by Cooper pairing is possible. These processes are examined in detail in Refs. 2 and 3 which carry out theoretical and experimental investigations of a continuous crossover from a tunnel *S–I–N*-contact to a no-barrier *S–N*-contact.

The characteristics may also be affected by the proximity effect which generates superconducting properties on the normal bank of the contact due to the finite transparency of the barrier. This was manifested most clearly in studies of substances with heavy fermions when the Josephson effect and Shapiro steps were observed in the initially fabricated *S–I–N*-contacts.[4,5]

The *I*-layer in the *S–I–N*-contact makes it possible to generate a relative shift in the chemical potentials of the superconductor and the normal metal by producing a potential difference at this layer. This can also be achieved by constriction, thereby producing a contact of smaller area. The properties of such an *S–c–N*-contact have been discussed in Refs. 6, 7. In a number of minor respects these differ from the *S–I–N*-characteristics.

The present study demonstrates that this does not exhaust the kinds of behavior of the *S–N*-contact. By analyzing the characteristics of a point *S–I–N*-contact we discover that it is possible to obtain $I(V)$ curves with a sharp inflection even at high relative temperatures of $t = T/T_c > 0.5$.

The layout of the article is as follows. The experimental technique is first described and the experimental results are provided. An amorphous $NiZr_2$ alloy was used as the superconductor. The superconducting transition in the amorphous alloys of transition metals[8–10] has certain specific features. First, the transition can be extraordinarily narrow with a width of $\delta T_c \approx 4$–5 mK (Ref. 11). Such a narrow width of $\delta T_c/T_c \approx 10^{-2}$ has been achieved previously only in carefully-fabricated, ultra-clean single crystals. This property of the amorphous metal results from the lack of macroscopic structural defects. Moreover a high degree of homogeneity of the composition on scales exceeding the coherence length ξ is required for its implementation. The value of ξ in this alloy has been repeatedly measured.[9–13] It is approximately 60 Å.

The next section presents a microscopic model of the *S–I–N*-contact that takes the proximity effect into account, yet is limited solely to one-particle tunneling processes.[14,15] A comparison of this model to experiment makes it possible to identify the principal causes of discrepancies and to formulate a direction for searching for an adequate explanation of the experiment.

In the last section we propose a model that we believe explains the experimental curves. This assumes that a thin surface superconducting layer is induced in the aluminum and there is an increase in the distance over which normal electrons will tunnel. The tunneling probability is nonzero only on the Fermi-level which contains an intermediate state manifested as a Cooper pair. It is likely that both the *I*-layer and constriction must occur simultaneously for such a model to be realized. We have therefore tentatively labeled such a contact a S–I_c–N-contact.

2. EXPERIMENT

An amorphous ribbon close to $NiZr_2$ in composition, which has been extensively studied,[9–13,16] was selected as the test specimen. The initial ribbon from which the specimens were cleaved had the following parameters: Ni concentration: 34 at.%, thickness: approximately 20 micrometers; resistivity at room temperature $\rho = 170$ $\mu\Omega\cdot$cm, $\rho_{4.2\,K}/\rho = 1.057$, and density 7.06 g/cm^3. $T_c = 2.46$ K, $\delta T_c \leqslant 4$–5 mK. No additional thermal treatments were used on the ribbon after quenching.

The properties of a Al–Al_2O_3–$NiZr_2$ tunnel point contact were investigated. The aluminum point was fabricated from a chemically-clean wire of diameter .25 mm by chemical etching followed by oxidation. The point radius thus obtained was approximately 0.5 μm. The mechanical system

 0038-5646/89/100813-05$04.00

used to deliver the point to the specimen was capable of generating graduated increments of the order of 0.01 μm. The normal resistivity R of the tunnel junctions lay in the 100–10 kΩ range. The "clean" limit with a path length $l_N \gg d$ is reliably achieved on the aluminum side of the contact, while the "dirty" limit with a path length $l_S \ll d$ is achieved on the amorphous alloy side. Estimates of contact dimensions d using expressions for both limits relating the resistance R to the path length and the transparency coefficient η, respectively

$$R=\eta^{-1}\rho l/d^2, \quad R=\eta^{-1}\rho/d,$$

show that in the no-barrier case ($\eta = 1$) it was necessary to assume that $d \leqslant 1$ Å holds. This means that the contact will reliably have a barrier with $\eta \leqslant 0.1$. We shall return to the estimation of η at the end of the paper.

The superconducting transition temperature was measured independent of the tunnel experiment using a four-point scheme with clip-on contacts. The narrow superconducting transition made it possible to achieve a better than 1% accuracy in determining the relative temperature $t = T/T_c$ which was used to record the characteristic.

Figure 1 provides a representative family of $I(V)$ curves for one of the contacts. It is clear that even with large values of t a clearly detectable bend appears in the curves. The voltage V_t at which the bend is observed is compared in Fig. 2 to a temperature plot of the gap width in BCS theory. This comparison provides sufficient grounds for identifying eV_t with the gap width $\Delta(t)$ at this temperature, at least with a certain degree of accuracy.

As an illustration of the discussion below Fig. 3 provides a comparison of one of the experimental curves to a curve calculated by the formula

$$I(V)=\frac{1}{eR}\int_{\Delta}^{\infty}\frac{\varepsilon\, d\varepsilon}{(\varepsilon^2-\Delta^2)^{1/2}}\left[f\left(\frac{\varepsilon-eV}{T}\right)-f\left(\frac{\varepsilon}{T}\right)\right], \qquad (1)$$

where ε is the energy relative to the Fermi level, while $f(x) = (1+e^x)^{-1}$ is the Fermi distribution function. The gap Δ was selected in the calculation so that Δ/e coincides with the voltage V_t at which the inflection appears on the experimental curve, while the normalization constant R was selected so that the contact resistance R when $\Delta = 0$ is equal to the resistance measured for $T > T_c$. Expression (1) was written down assuming that all current was produced by tunneling of one-particle excitations to states lying above the energy gap of the superconductor, that the tunneling probability is independent of energy and that the proximity effect is not manifested in the state density on either the normal or the superconducting banks of the contact. It is clear from Fig. 1 that at least one of these assumptions was not valid in the experiments described here.

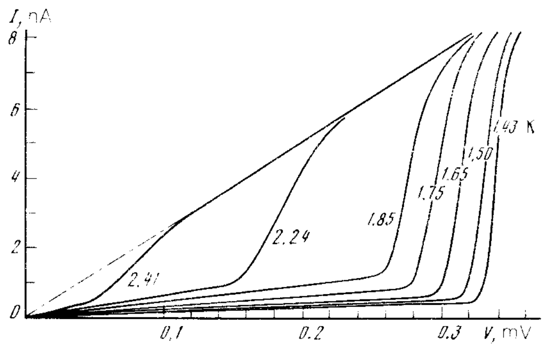

FIG. 1. Family of I-V characteristics of a contact with normal resistance $R = 40$ kOhms.

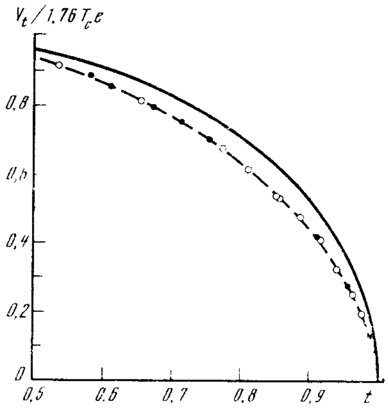

FIG. 2. Position of the inflection V_t on the $I(V)$ curves plotted as a function of the reduced temperature t. The different designations on the points correspond to different contacts. The solid curve represents the width of the superconducting gap in BCS theory plotted as a function of the reduced temperature.

Normally the $I(V)$ curves discussed here were observed only with a freshly fabricated point. The evolution occurring with the curves from repeated usage of a point is demonstrated in Fig. 4. The recording sequence is indicated by numbers 1–5 near the curves. After each subsequent curve plot at 1.3 K, the point was removed from the specimen, the instrument was heated to 4.2 K, and the point was then reapplied so that a resistance less than that obtained in the preceding measurement was achieved; the vertical scale was than normalized to the resistance level obtained here and the next reading was taken after cooling to 1.3 K. Figure 4 shows a gradual crossover to the classical characteristic described by the integral (1).

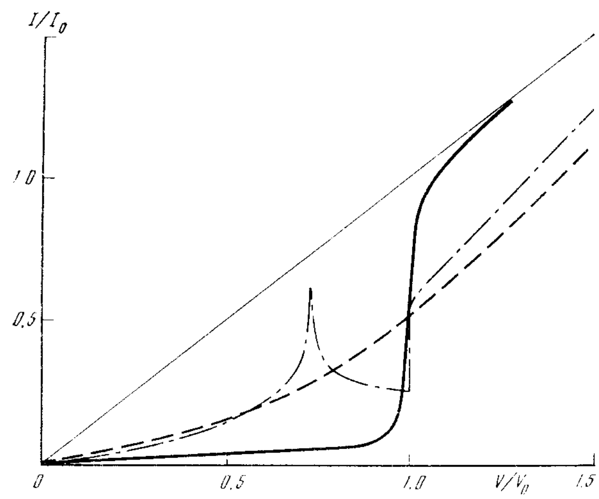

FIG. 3. Comparison of an experimental $I(V)$ curve (bold solid curve) with a simple one-particle model [formula (1), dashed curve] and a model accounting for the proximity effect (dot and dash curve, see below, section 3). Here we have $I_0 = V_0/R$, $eV_0 = \Delta_{BCS}(T)$ for the experimental curve and model (1), $eV_0 = \Delta_{BCS}(T) + \Omega$ for the model taking account of the proximity effect, $t = 0.52$.

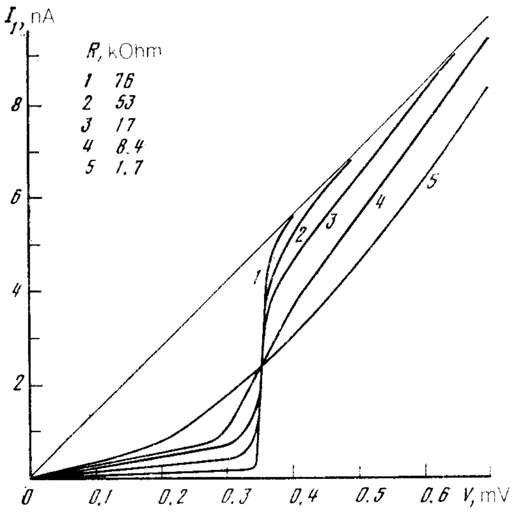

FIG. 4. Change in the shape of the $I(V)$ curve of a contact upon successive applications of the point $i = 1$–5 and a fixed temperature $t = 0.52$. Scale I_1 corresponds to curve 1. We have $I_i = I_1 R_1 / R_i$ for curves with $i = 2$–5.

3. THE PROXIMITY EFFECT IN AN *S–I–N*-CONTACT

A microscopic model of the proximity effect in a superconductor-normal metal system that self-consistently accounts for the spatial homogeneity of the order parameter Δ has been analyzed in Refs. 14 and 15 for the case of random transparency of the N–S-boundary. This model assumes that the dirty limit conditions hold for the N- and S-metals, the critical temperature of the N-metal T_{cN} is equal to zero and that the N- and S-materials have different transport properties. The system geometry plays an important role, as demonstrated in Ref. 14. The excitation spectrum in the N-region is gapless for the case of a plane junction of two bulk metals ($d_N \gg \xi_N$, $d_S \gg \xi_S$, where $d_{N,S}$ and $\xi_{N,S}$ are the thicknesses and coherence lengths of the N- and S-layers, respectively), i.e., the state density $\eta(\varepsilon)$ is nonzero at all energy values. In the case of a thin N-layer ($d_N \ll \xi_N$) the excitation spectrum of a normal metal will contain the induced energy gap $\Omega < \Delta(T)$. The gap Ω will depend on two parameters, γ_M and γ_B, characterizing the degree of spatial inhomogeneity of the superconducting properties of the N–S-sandwich and the effective transparency of the N–S-boundary, respectively:

$$\gamma_M = \frac{\rho_S \xi_S}{\rho_N \xi_N} \frac{d_N}{\xi_N}, \tag{2}$$

$$\gamma_B = \frac{R_b}{\rho_N \xi_N} = \frac{2}{3} \frac{l_N/\xi_N}{\langle xQ/P \rangle} \frac{d_N}{\xi_N}, \tag{3}$$

where $\rho_{N,S}$ are the resistivities of the N- and S-metals in the normal state, R_b is the product of the resistance of the N–S-boundary and its area, Q and P are the transmission and reflection coefficients for the potential barrier at the N–S-boundary, x is the relative value of the projection of electron momentum onto the normal to the N–S-boundary, and the angle brackets represent integration over the sphere. The identity $\eta = \langle xQ/P \rangle$ holds with a small transparency coefficient η.

We examine in greater detail the case of a thin normal layer $d_N \ll \xi_N$. When the parameter γ_M has sufficiently small values ($\gamma_M \ll 1 + \gamma_B$) the energy dependence of the state density in the N-region, $\eta_N(\varepsilon)$, has two singularities. The first singularity corresponds to the energy gap Ω induced in the N-metal and depends on the value of the parameter γ_B. For γ_B 1 (low effective transparency of the N–S-boundary) the energy gap is small:

$$\Omega = (\pi/\gamma^* \gamma_B)\Delta(T), \tag{4}$$

where $\gamma^* = 1.78$ is Euler's constant. For $\gamma_B \ll 1$ (high effective transparency) the gap Ω is approximately equal to $\Delta(T)$. The second singularity in the state density of a normal metal occurs for $\varepsilon = \Delta(T)$, i.e., it is related to the size of the superconductor gap. In this case for $\gamma_M \ll 1 + \gamma_B$ the effect of the normal metal on superconductivity in the S-region is negligible and the state density in the S-layer is

$$n_S(\varepsilon) = n_{S_0} \operatorname{Re}\{\varepsilon[\varepsilon^2 - \Delta^2(T)]^{-1/2}\},$$

i.e., the same state density as in the BCS model for a spatially-homogeneous superconductor (n_{S_0} is the normal state density).

Taking the finite value of the parameter γ_M into account will cause a smearing of these singularities of the state densities of the N- and S-metals and will cause them to shift towards lower energy levels. This shift results from the suppression of the order parameter of the superconductor near the N–S-boundary due to the diffusion of normal excitations from the N-metal.

Figure 5 provides the state densities in the normal and superconducting regions of an N–S-sandwich calculated within the framework of this model for a number of values of γ_M and γ_B for illustrative purposes. It is clear that the energy gap Ω is induced in the N-metal. Moreover the state density in the S-region of the N–S-sandwich changes radically with an increasing parameter γ_M (see Fig. 5b). The gap may decrease from $\Delta(T)$ at $\gamma_M = 0$ to Ω.

Knowledge of the state densities in the N- and S-regions of the sandwich permits calculation of the one-particle tunnel current of the S–I–N-contact within the framework of the standard tunnel Hamiltonian scheme. This scheme takes into account only the contribution of first-order processes in the transparency of the N–S-boundary. In Fig. 3 the dot-dash curve represents one of the characteristics calculated in this manner for comparison to the experimental curve. This curve was plotted for the same relative temperature $t = 0.52$ as the experimental curve for $\gamma_M = 0$ and $\gamma_B = 10$. Unity on the X-axis corresponds to a voltage $eV = \Delta(T) + \Omega$. The additional singularity at the voltage $eV = \Delta(T) - \Omega$ is analogous to the familiar singularity for standard S_1–I–S_2 tunnel structures with different banks ($\Delta_1 \neq \Delta_2$) when $T \neq 0$ holds.

It is important to note that in spite of the induced superconductivity in the N-metal there is no Josephson supercurrent in this model when the potential difference vanishes between the N- and S-banks of the contact, since the boundary conditions at the N–S-boundary[15] cause the phases of the order parameters in the N- and S-layers to coincide.

4. DISCUSSION

A comparison of the experimental and theoretical curves in Fig. 3 reveals two significant characteristics: the absence of activation current on the experimental curve for $eV < \Delta$ and the rapid assumption of a normal characteristic

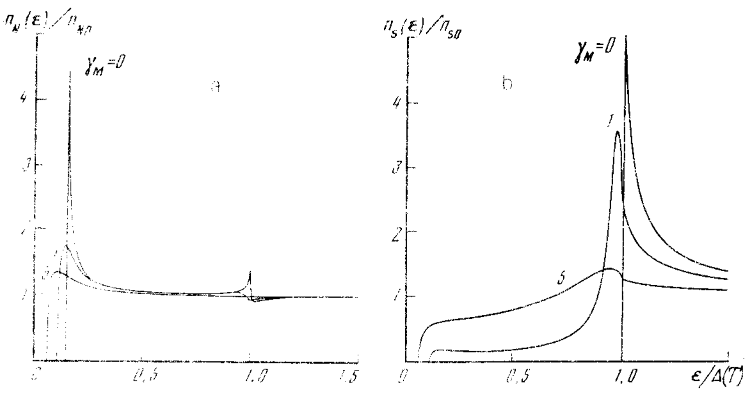

FIG. 5. State densities of the normal (a) and superconducting (b) banks of a contact for a number of parameters γ_M (indicated near the curves) for $\gamma_B = 10$ (η_N, η_S are the normalized state densities of the banks).

($I_N = V/R$) when $eV < \Delta$ holds. We begin with a discussion of the first feature.

The activation current will be suppressed naturally if induced superconductivity occurs at the N-bank: the current I is proportional to $\exp[-(\Delta+\Omega)/T]$ rather than $\exp[-\Delta/T]$. We discuss this possibility with application to our experiment. In the ideal case of a no-barrier S–N-contact of bulk N- and S-metals, gapless superconductivity will occur in the N-metal near the contact plane, while the state density at the Fermi level drops substantially. We have two additional factors compared to this ideal case. The first is the presence of a barrier which impedes the onset of superconductivity. A high value of the parameter γ_B corresponds to low barrier transparency in the theory discussed in the preceding section; its role is reflected in (4). However according to (3) even with a high coefficient of reflection off the barrier, i.e., when $\eta \ll 1$ holds, for $d_N/\xi_N \ll 1$ it is possible that $\gamma_B \ll 1$ will be valid.

The second factor is the finite size of the contact. Equation (4) was written for a plane S–N-contact. In the three-dimensional case the contact dimensions d can play the role of the small parameter d_N. The smallness of this parameter can enhance the effect of the S-bank of the contact on the N-bank.

Therefore these two factors, the small barrier transparency and the small contact dimensions d, have opposing effects on the proximity effect. Any state of the N-bank from a normal state through a superconducting state with a gap is likely to be possible in these conditions.

Generally in order to suppress the current in the case of low voltages when $eV < \Delta(T)$ holds it is sufficient to reduce the state density within a certain neighborhood ($|\varepsilon| \leqslant \Omega$) of the Fermi-level of a normal metal. Such a drop will occur even with gapless superconductivity, since the difference between gap and gapless superconductivity is only quantitative in this sense. The experiments discussed here cannot distinguish between the last two possibilities. Only a small state density of $\beta = n_N(\varepsilon)/n_N \ll 1$ in the neighborhood of the Fermi-level and a superconducting condensate on the N-bank are required for the explanation of the features of the experimental curves provided below.

The evolution of the characteristics shown in Fig. 4 can be considered to be a confirmation of the role of the contact area. The contact area d^2 grows with each subsequent application of the point (compare to Ref. 3). This is accompanied by a reduction in the width of the gap or pseudogap Ω; in the case of gapless superconductivity the depth $1-\beta$ of the minimum may also drop.

The characteristic energy Ω appearing in the state density of the N-bank gives rise, however, to another fundamental difficulty. It is necessary for $\Omega \approx \Delta(T)$ to hold in order to achieve effective current suppression for $eV < \Delta(T)$. In this case one-particle tunnel current must appear when $eV = \Omega + \Delta(T) \approx 2\Delta(T)$ holds, and the inflection on the $I(V)$ curve must be identified with $2\Delta(T)$. This would mean that the agreement with BCS theory in Fig. 2 is incidental and that $\Delta(T) \approx 1/2\Delta_{BCS}(T)$ holds. Such a possibility is extremely unlikely and this makes it necessary to seek out an explanation for the observed characteristics that goes beyond the framework of the one-particle approximation.

Therefore we assume for definiteness that a superconducting region with an induced gap $\Omega \approx \Delta(T)$ arose at the point due to the finite barrier transparency γ_B^{-1} and the small contact area d^2 (see the scheme in Fig. 6). This region forms an additional barrier to normal electrons of energies $|\varepsilon| < \Omega$ which is responsible for the low current at low voltages. However for $eV \approx \Delta(T)$ a new Cooper pair tunneling channel through the I-layer is opened up. This channel operates in the following manner.

An electron of energy ε from the normal metal at the boundary of the S_{ind}-region, by binding to the $-\varepsilon$ hole, transforms into a Cooper pair at the Fermi-level; the pair, by

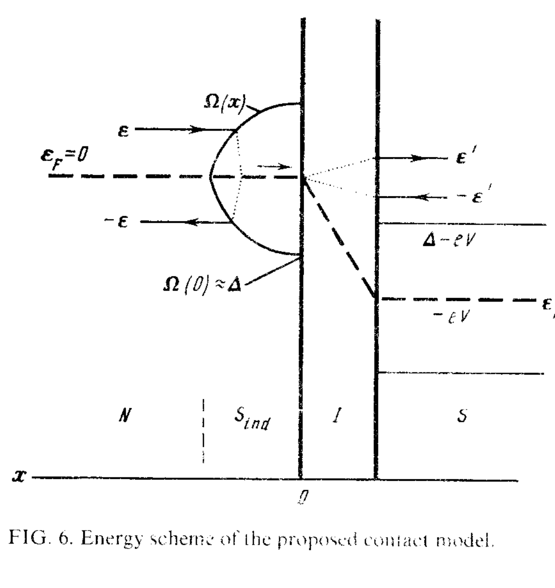

FIG. 6. Energy scheme of the proposed contact model.

tunneling through the dielectric, is transformed into two excitations of energies ε' and $-\varepsilon'$ with $0<\varepsilon'\leqslant eV-\Delta(T)$. The latter inequality is responsible for the final slope of the characteristic for $V>V_t$, since the number of possible final states of the normal excitations in the S-region grows with increasing $V-V_t$. The first stage of this process is Andreev reflection, while the second is two-particle tunneling. Both have been accounted for in Refs. 17–19, although without assuming induced superconductivity in the N-metal.

We now focus on the right side of the characteristics for the case for $eV>\Delta$. Two-particle tunneling is characterized by excess current $\delta I=I-I_N>0$ when $eV>\Delta(T)$ holds.[3,6,7,17-20] On the other hand the difference $\delta I<0$ is valid in the case of one-particle tunneling in an S–I–N-contact in the same manner as in an S–c–N-contact, where the crossover to a normal $I_N(V)$ characteristic is extended and when $eV\approx(2\text{–}4)\Delta(T)$ holds, $|\delta I|$ is still rather substantial. Hence the rapid crossover of the $I(V)$ curve to a normal characteristic requires a special explanation.

The explanation is also related to the small area of the contact. Since the path length l_S in an amorphous material is of the order of the interatomic distance, with virtually any contact dimensions d the following inequality holds:

$$d\gg l_S. \tag{5}$$

In these conditions the current density through the contact j in this approximation will be dependent on its area:

$$j=I/d^2=V/Rd^2=V/\rho d, \tag{6}$$

and with small d may exceed the depairing current[21]

$$j_p=en_{S0}D^{1/2}\Delta^{1/2},$$

(D is the diffusion coefficient). Indeed substituting $V=\Delta/e$ into (6) and using the relations $\rho=(e^2n_{S_0}D)^{-1}$ and $\xi=(D/\Delta)^{1/2}$ we obtain

$$j/j_p=\xi/d. \tag{7}$$

Therefore in a contact whose dimensions satisfy the inequalities

$$\xi>d\gg l, \tag{8}$$

where $eV\approx\Delta(T)$ holds the current density exceeds the critical value and a normal neighborhood of the contact results.

Relation (7) makes it possible to return to the issue of contact parameters. Assuming the condition $d\approx\xi\approx60$ Å is realized for curve 4 in Fig. 4 we obtain $\eta\approx0.03$ from $R=\rho/\eta d$. Consequently the dimensions d of all contacts having characteristics with a sharp bend (Fig. 1, curve 1 in Fig. 4, etc.) are of the order of 10 Å.

5. CONCLUSION

The following model of physical phenomena in the test contact is proposed based on the analysis carried out above.

A superconducting state is induced in the contact aluminum layer by virtue of the small contact dimensions ($d\approx10$ Å), in spite of the presence of an isolating barrier. As a result one-particle current is blocked at low voltages for $eV<\Delta$. For $eV\approx\Delta$ one-particle tunneling remains blocked, although there is also a rapid rise in current due to two-particle tunneling. The current approaches values of $I=\Delta/eR$ upon further growth of eV there is a current-induced breakdown of superconductivity in the vicinity of the contact due again to smallness of the contact, $d<\xi$, and smallness of the path length in the amorphous material ($l<d$).

Of course the proposed model requires theoretical substantiation. At least three clear-cut questions can be addressed to the theory: To what degree may smallness of the contact area compete with the insulating layer in the induction of superconductivity and does smallness of l or ξ in the superconductor play any role in this process; how are the parameters in an N–S–I–S-sandwich with thin internal S- and I-layers to be selected to achieve a noticeable contribution of two-particle tunneling and how do depairing processes affect the I-V characteristic of the contact with a short path length in which the inequality $\xi>d\gg l$ holds?

The authors are grateful to S. L. Pryadkin for methodological advice in developing the setup and to I. O. Kulik for stimulating discussion.

[1] L. Solymar, *Superconductive Tunneling and Applications*, Chapman and Hall, London (1972).
[2] G. E. Blonder, M. Tinkham, and T. M. Klapwijk, Phys. Rev. B. **25**, 4515 (1982).
[3] G. E. Blonder and M. Tinkham, Phys. Rev. B. **27**, 112 (1983).
[4] S. Han, K. W. Ng, E. L. Wolf *et al.*, Phys. Rev. B. **32**, 7567 (1985).
[5] S. Han, K. W. Ng, E. L. Wolf *et al.*, Phys. Rev. Lett. **57**, 238 (1986).
[6] S. N. Artemenko, A. F. Volkov, and A. V. Zaitsev, Sol. St. Comm. **30**, 771 (1979).
[7] A. V. Zaytsev, Zh. Eksp. Teor. Fiz. **78**, 221 (1980) [Sov. Phys. JETP **51**, 111 (1980)].
[8] S. J. Poon, *Amorphous Metallic Alloys*, Ed. F. E. Luborsky, Butterworths, London (1983).
[9] M. Tenhover and W. L. Johnson, Phys. Rev. B. **27**, 1610 (1983).
[10] Z. Altounian and J. O. Strom-Olsen, Phys. Rev. B. **27**, 4149 (1983).
[11] S. J. Poon, Phys. Rev. B. **27**, 5519 (1983).
[12] F. P. Missell and J. E. Keem, Phys. Rev. B. **29**, 5207 (1984).
[13] O. Laborde, A. Ravex, J. C. Lasjaunias, and O. Be'thoux, J. Low Temp. Phys. **56**, 461 (1984).
[14] A. A. Golubov and M. Yu. Kupriyanov, J. Low Temp. Phys. **70**, 83 (1988).
[15] A. A. Golubov and M. Yu. Kupriyanov, Zh. Eksp. Teor. Fiz. **96**, 1420 (1989) [Sov. Phys. JETP **96**, this issue (1989)].
[16] G. A. Abrosimova, A. S. Aronin, V. F. Gantmakher *et al.*, Fiz. Tverdogo Tela, **30**, 1424 (1988) [Sov. Phys. Solid State. **30**, 822 (1988)].
[17] A. L. Shelankov, Fiz. Tverdogo Tela **26**, 1615 (1984) [Sov. Phys. Solid State **26**, 981 (1984)].
[18] A. V. Zaytsev, Zh. Eksp. Teor. Fiz. **86**, 1742 (1984) [Sov. Phys. JETP**59**, 1015 (1984)].
[19] G. B. Arnold, J. Low Temp. Phys. **59**, 143 (1985).
[20] S. I. Dorozhkin, Zh. Eksp. Teor. Fiz. **79**, 1025 (1980) [Sov. Phys. JETP **52**, 520 (1980)].
[21] K. Maki, Progr. Theor. Phys. **29**, 333 (1963).

Translated by Kevin S. Hendzel